Inorganic Chemistry
Article
Cite This: Inorg. Chem. 2018, 57, 5108−5113
pubs.acs.org/IC

Synthesis, Structure, and Properties of the Layered Oxyselenide $Ba_2CuO_2Cu_2Se_2$

Wenmin Li,[†,‡] Zhaoming Fu,[†] Xiancheng Wang,*[,†] Jun Zhang,[†,‡] Min Liu,[†,‡] Jianfa Zhao,[†,‡] Meiling Jin,[†,‡] Guoqiang Zhao,[†,‡] Guangyang Dai,[†,‡] Zheng Deng,[†] Sijia Zhang,[†] Shaomin Feng,[†] Zhiwei Hu,[§] Qingzhen Huang,[∥] Hongji Lin,[⊥] Chien-Te Chen,[⊥] Yifeng Yang,*[,†,‡,#] and Changqing Jin*[,†,‡,#]

[†]Beijing National Laboratory for Condensed Matter Physics, Institute of Physics, Chinese Academy of Sciences, Beijing 100190, China

[‡]School of Physics, University of Chinese Academy of Sciences, Beijing 100190, China

[§]Max Plank Institute for Chemical Physics of Solids, Nöthnitzer Strasse 40, D-01187 Dresden, Germany

[∥]Center for Neutron Research, National Institute of Standards and Technology, Gaithersburg, Maryland 20899-6102, United States

[⊥]National Synchrotron Radiation Research Center (NSRRC), 101 Hsin-Ann Road, Hsinchu 30076, Taiwan

[#]Collaborative Innovation Center of Quantum Matter, Beijing 100190, China

Supporting Information

ABSTRACT: A new layered oxyselenide, $Ba_2CuO_2Cu_2Se_2$, was synthesized under high-pressure and high-temperature conditions and was characterized via structural, magnetic, and transport measurements. It crystallizes into space group $I4/mmm$ and consists of a square lattice of $[CuO_2]$ planes and antifluorite-type $[Cu_2Se_2]$ layers, which are alternately stacked along the c axis. The lattice parameters are obtained as $a = b = 4.0885$ Å and $c = 19.6887$ Å. The Cu−O bond length is given by half of the lattice constant a, i.e., 2.0443 Å. $Ba_2CuO_2Cu_2Se_2$ is a semiconductor with a resistivity of ∼18 mΩ·cm at room temperature. No magnetic transition was found in the measured temperature range, and the Curie−Weiss temperature was obtained as −0.2 K, suggesting a very weak exchange interaction. The DFT+U_{eff} calculation demonstrates that the band gap is about 0.2 eV for the supposed antiferromagnetic order, and the density of state near the top of the valence band is mainly contributed from the Se 4p electrons.

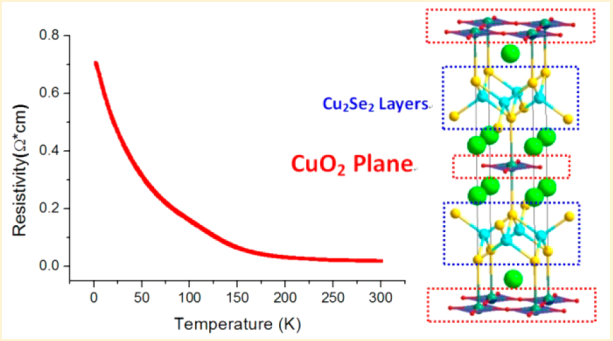

INTRODUCTION

The discovery of high-temperature cuprate superconductors has generated great interest in exploring new cuprate superconductors and studying the high-temperature superconducting mechanism since 1986,[1−5] and the current reports of iron-based superconductors have rekindled global interest.[6−10] The cuprate and iron pnictide families of high-T_c compounds contain a superconducting square-lattice plane of $[CuO_2]$ and antifluorite layers of $[Fe_2As_2]$, respectively. Because the lattice of the antifluorite layer can be changed through deformation of the tetrahedron of $M'X_4$ (M' is a 3d metal, and X is pnicogen or chalcogen), it is easy to design a geometry and charge-compatible structure that consists of both rock-salt and antifluorite layers and build up new materials with novel properties.[11] A prominent example is the new oxypnictides of $[Ca_{n+1}(Sc,Ti)_nO_y]Fe_2As_2$ ($n = 3−5$)[12] and $Sr_3Sc_2O_5Fe_2As_2$,[13] where the superconducting $[Fe_2As_2]$ layers are sandwiched by thick rock-salt layers. On the basis of the antifluorite layer of $[Cu_2S_2]$, oxysulfides with the formula $(Sr_{n+1}M_nO_{3n-1})Cu_2S_2$ ($n = 1−3$; M = Cr, Mn, Fe, Co, Zn, and Cu) have been synthesized and systematically studied.[14−18] The intriguing oxysulfide is $Sr_2CuO_2Cu_2S_2$ because it consists of $[CuO_2]$ planes and is considered to be a candidate for the superconductor.[16] For oxyselenides, the compounds of $Sr_2MO_2Cu_2Se_2$ (M = Co and Mn) are currently reported,[19] and $Sr_2CoO_2Cu_2Se_2$ was studied as a potential thermoelectric material.[20] Another interesting material is $Na_{1.9}Cu_2Se_2Cu_2O$,[21] which features alternately stackable layers of $[Cu_2Se_2]$ and $[Cu_2O]$ and presents a metallic state. However, it should be noted that the $[Cu_2O]$ plane in $Na_{1.9}Cu_2Se_2Cu_2O$ is the reversed atom site of the $[CuO_2]$ plane in general cuprate oxidation compounds.

Here, we report a new oxyselenide, $Ba_2CuO_2Cu_2Se_2$, which contains a square lattice of $[CuO_2]$ planes and antifluorite $[Cu_2Se_2]$ layers. It is a semiconductor with a low resistivity at

Received: January 19, 2018
Published: April 9, 2018

DOI: 10.1021/acs.inorgchem.8b00171
Inorg. Chem. 2018, 57, 5108−5113

room temperature. The Curie–Weiss temperature T_{CW} is very close to zero, indicating a very weak exchange interaction. The electronic structure is calculated, and the results show that the $[Cu_2Se_2]$ layers dominate the density of state (DOS) near the top of the valence band.

EXPERIMENTS AND CALCULATIONS

The polycrystalline sample of $Ba_2CuO_2Cu_2Se_2$ was synthesized under high-pressure and high-temperature conditions using BaSe, CuO (99.9%), and Cu (99.9%) powders as the starting materials. The BaSe precursors were prepared by reacting high-purity Ba blocks and Se powders at 700 °C for 20 h in an evacuated quartz tube. The tube was sealed under a vacuum (10^{-4} Pa) and heated in a muffle furnace. The starting materials were mixed according to the element ratio of stoichiometric $Ba_2CuO_2Cu_2Se_2$, pressed into a pellet, and then subjected to high-pressure synthesis under 5.5 GPa pressure and 1000 °C for 40 min in a cubic-anvil-type high-pressure facility, the details which have been reported in ref 22. Because of the air-sensitive precursors of Ba, Se, and BaSe, all of the processes prior to the high-pressure synthesis were performed in a glovebox filled with argon gas, with the H_2O and O_2 contents less than 1 ppm. In addition, our attempt to synthesize $Ba_2CuO_2Cu_2Se_2$ at ambient pressure was not successful.

Powder X-ray diffraction (XRD) was performed using a Rigaku Geigerflex powder diffractometer with a copper target at room temperature. Neutron powder diffraction (NPD) was carried out at the Center for Neutron Research, National Institute of Standards and Technology, at both room temperature and 3 K, with a wavelength of 1.5397 Å. Rietveld refinements on the powder XRD and NPD patterns were performed using the *GSAS* software package. Electrical resistivity measurements were carried out with a Physical Property Measurement System (Quantum Design). The direct-current magnetic susceptibility was measured using a vibrating-sample magnetometer (Quantum Design) under a magnetic field of 3 T. Soft X-ray absorption spectroscopy (XAS) at the Cu $L_{2,3}$-edges was measured at beamline BL11A of the NSRRC in Taiwan.

Density functional theory (DFT) with the full-potential augmented-plane-wave method was used to study the electronic structures of $Ba_2CuO_2Cu_2Se_2$, as implemented in the *WIEN2K* code.[23] For the exchange-correlation functional, the Perdew–Burke–Ernzerhof form was adopted. An empirical value of U_{eff} = 7 eV was used as is for cuprate superconductors.[24] The maximum modulus of the reciprocal vectors K_{max} was chosen such that $R_{MT}K_{max}$ = 8.0. The first Brillouin zone was sampled using a 10 × 10 × 10 k mesh.

RESULTS AND DISCUSSION

Figure 1a shows the NPD pattern of $Ba_2CuO_2Cu_2Se_2$ collected at room temperature. All of the peaks can be indexed with a tetragonal structure with the lattice parameters $a = b$ = 4.0885 Å and c = 19.6887 Å. Here, the structure of $Ba_2ZnO_2Zn_2As_2$,[25] which crystallizes into space group $I4/mmm$ (No. 139), is adopted as an initial model for the Rietveld refinement. In the process of refinement, if the occupancy rates are released to be fitted, the lowest occupancy rate is 0.975(10) for the Cu(2) site (shown in Table S1), which demonstrates that the elementary ratio in the synthesized compound is very close to that of the stoichiometric $Ba_2CuO_2Cu_2Se_2$. Thus, here, the occupancy rates for all of the elements are fixed at 1. The refinement smoothly converges to R_{wp} = 5.3%, R_p = 4.4%, and χ^2 = 1.1. The XRD pattern is shown in Figure S1. Table 1 shows a summary of the crystallographic data from NPD, and the crystal structure is presented in Figure 1b. $Ba_2CuO_2Cu_2Se_2$ consists of $[CuO_2]$ planes and antifluorite $[Cu_2Se_2]$ layers, which are alternately stacked along the c axis and separated by Ba ions. In the structure, there are two Cu sites. The Cu(1) site with (0.5, 0, 0.25) locates in the $[Cu_2Se_2]$ layer; while the Cu(2) site with

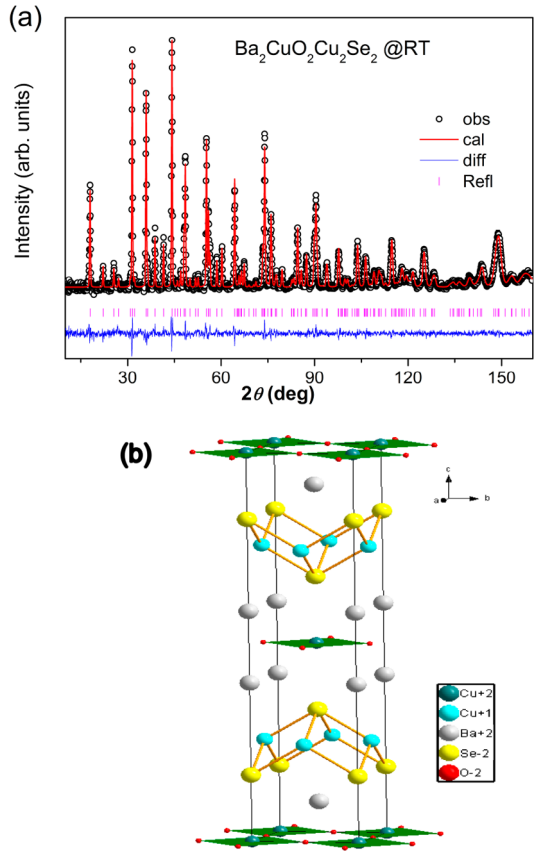

Figure 1. (a) NPD pattern at room temperature for $Ba_2CuO_2Cu_2Se_2$ and its Rietveld refinement. Observed (black circles), calculated (red line), and difference (blue line) profiles are shown together with the allowed Bragg reflections (ticks). (b) Crystal structure of $Ba_2CuO_2Cu_2Se_2$.

Table 1. Summary of the Crystallographic Data for $Ba_2CuO_2Cu_2Se_2$ of NPD at Room Temperature

Phase Data						
formula: $Ba_2CuO_2Cu_2Se_2$						
space group: $I4/mmm$ (No. 139)						
a = 4.0885(2) Å, c = 19.6887(4) Å						
R_{wp} = 5.3%, R_p = 4.4%, χ^2 = 1.1						
Atomic Parameters						
site	Wyckoff	x	y	z	occupany	$100U_{iso}$
Cu(1)	4d	$^1/_2$	0	$^1/_4$	1	1.77(6)
Cu(2)	2a	0	0	0	1	0.90(6)
Ba	4e	$^1/_2$	$^1/_2$	0.09165(14)	1	0.69(6)
Se	4e	0	0	0.17504(9)	1	0.81(5)
O	4c	$^1/_2$	0	0	1	1.28(7)

(0, 0, 0) is in the $[CuO_2]$ plane. Generally, in the oxypnictide or oxychalcogenide compounds, two different atoms (M and M′) of the transition metal can locate in the positive block of salt-rock layers of $[A_2MO_2]^{2+}$ (A denotes an alkali-earth metal) and the negative antifluorite layers $[M'_2X_2]^{2-}$ (X denotes pnicogen or chalcogen), respectively. The valence of M usually is 2+, while M′ is 2+ and 1+ for the oxypnictides and oxychalcogenides, respectively. That is, for $Ba_2CuO_2Cu_2Se_2$, Cu(2) should be bivalent, with the $3d^9$ configured, while Cu(1) might be monovalent, with the 3d orbital fully filled. Also, we can evaluate the oxidation state of Cu from the method of bond

DOI: 10.1021/acs.inorgchem.8b00171
Inorg. Chem. 2018, 57, 5108–5113

valence sum (BVS). Table 2 presents the bond lengths. The calculated BVS value of Cu(2) is 1.53 and that of Cu(1) 1.03. It

Table 2. Structure Parameters of $Ba_2CuO_2Cu_2Se_2$ Refined from NPD Measured at Room Temperature and BVS Values for the Cu(1) and Cu(2) Ions

parameter	value
Cu(2)−O (×4)	2.0443(1) Å
Cu(2)−Se (×2)	3.4465(12) Å
Cu(1)−Se (×4)	2.5212(4) Å
Ba−O (×4)	2.7282(3) Å
∠O−Cu(2)−O	90.0°
∠Cu(2)−O−Cu(2)	180.0°
∠Se−Cu(1)−Se (×2)	108.3°
∠Se−Cu(1)−Se (×4)	110.0°
BVS[Cu(1)][a]	1.03
BVS[Cu(2)][a]	1.53

[a]The BVS values (V_i) were calculated using the formula $V_i = \sum_j S_{ij}$, where $S_{ij} = \exp[(r_0 - r_{ij})/0.37]$. To evaluate the oxidation state of Cu, the value of $r_0 = 1.679$ is used for coordinated O atoms and $r_0 = 2.02$ for coordinated Se atoms.

is noted that, for the Cu(2) site with four coordinated O atoms and two coordinated Se atoms, the oxidation state of Cu(2) is undervalued by the BVS method because of the influence of the seriously extended Cu−O bond. Similar results have been reported in $Ba_2ZnO_2Ag_2Se_2$ (for Zn, the BVS is 1.35),[26] $Ba_2CoO_2Ag_2Se_2$ (for Co, the BVS is 1.287), and $Ba_2MnO_2Ag_2Se_2$ (for Mn, the BVS is 1.59).[27] For the oxidation state of Cu(1), the BVS value is coincident with the result analyzed from the view of the crystal structure.

To further study the oxidation state of Cu ions, XAS measurements were carried out. Figure 2a shows the Cu $L_{2,3}$-edge XAS of $Ba_2CuO_2Cu_2Se_2$, and the high-quality single-crystal sample of La_2CuO_4 with pure Cu^{2+} is used as the reference. The spectra are normalized in energy around 990 eV, where the absorption is featureless. The enlarged view of the L_3-edge spectra is displayed in Figure 2b. Peak A around 931.3 eV, which can be seen in both $Ba_2CuO_2Cu_2Se_2$ and La_2CuO_4, is assigned to a $2p^53d^{10}$ final state coming from a $2p^63d^9$ initial state,[28,29] demonstrating the existence of Cu^{2+} ions. Nearly no energy shift is observed at the L_3 edge, while the intensity of $Ba_2CuO_2Cu_2Se_2$ decreases strongly compared with the spectra of La_2CuO_4. The peak marked by the arrow around 934.8 eV is assigned to the $2p^53d^{10}4s^1$ final state for the Cu^+ ion, which is reported in Cu_2O and $LiCu_2O_2$.[30,31] Therefore, XAS measurements give unambiguous evidence for the existence of two oxidation states of Cu^{2+} and Cu^+ in $Ba_2CuO_2Cu_2Se_2$.

The temperature dependence of the resistivity of $Ba_2CuO_2Cu_2Se_2$ is shown in Figure 3. The resistivity increases with decreasing temperature, presenting semiconducting behavior. The inset shows $\ln(\rho)$ versus inverse temperature in the high-temperature region. By using the formula of $\rho \propto \exp(\Delta/2k_BT)$, where Δ is the semiconducting band gap and k_B is the Boltzmann constant, the resistivity curve can be fitted and the band gap Δ is evaluated to be 68 meV. It is noted that the resistivity at room temperature (ρ_r) is very low at about 18 mΩ·cm, which is very close to that of $Sr_2CoO_2Cu_2Se_2$ with a ρ_r value of about 11 mΩ·cm[19] and several orders lower than that of $Sr_2CoO_2Cu_2S_2$ ($\rho_r \sim 4000$ mΩ·cm).[15] In fact, most of oxyselenides are semiconductors, except the samples in which the antifluorite layers are charge-doped.[17] Taking

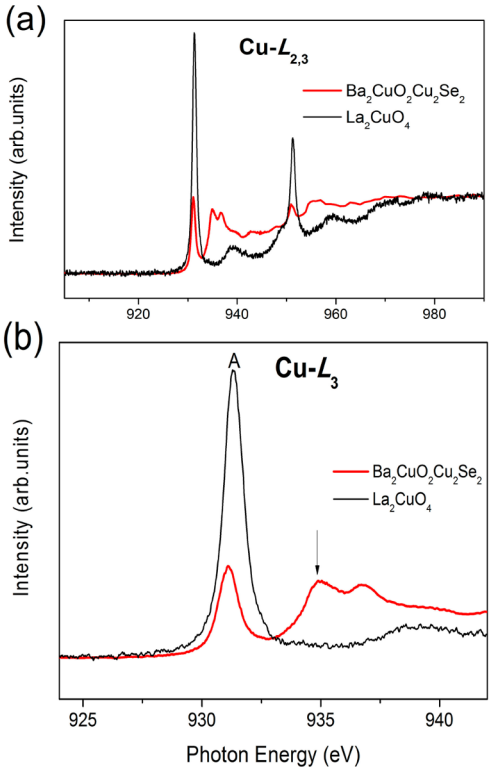

Figure 2. (a) Cu $L_{2,3}$-edge fluorescence yielding photoabsorption spectra of $Ba_2CuO_2Cu_2Se_2$ with the high-quality single-crystal sample La_2CuO_4 as a pure Cu^{2+} reference. (b) Enlarged view of L_3-edge XAS.

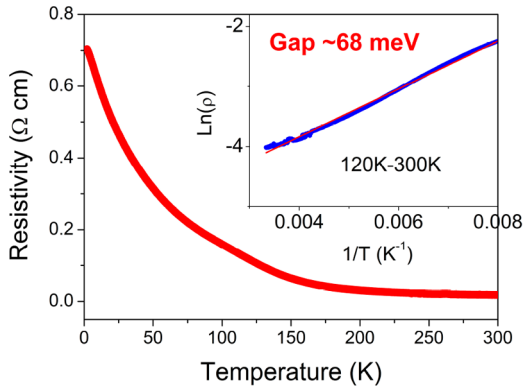

Figure 3. Temperature dependence of the resistivity $\rho(T)$ for the $Ba_2CuO_2Cu_2Se_2$ sample. The inset shows $\ln(\rho)$ versus inverse temperature.

$Bi_2YO_4Cu_2Se_2$ as an example, it is metallic with a ρ_r value of about 0.59 mΩ·cm because charge transfer happens between the $[Cu_2Se_2]$ and $[Bi_2YO_4]$ layers.[32] In addition, for these oxychalcogenides, the valence band or the band near the Fermi surface, determining the conduction behavior, is mainly derived from antifluorite layers.[17,20,32] Hereafter, we will also illustrate that it is the same for $Ba_2CuO_2Cu_2Se_2$.

Figure 4 displays the temperature dependence of the magnetic susceptibility for $Ba_2CuO_2Cu_2Se_2$ measured at 3 T. No anomaly can be found corresponding to the magnetic phase transition in the measured temperature range. The inverse susceptibility versus temperature is a straight line, demonstrating Curie−Weiss behavior in the paramagnetic region. When the line is fitted, the Weiss temperature T_{cw} is obtained to be −0.21 ± 0.06 K and an effective moment $\mu_{eff} \sim 1.01\ \mu_B$ per

DOI: 10.1021/acs.inorgchem.8b00171
Inorg. Chem. 2018, 57, 5108−5113

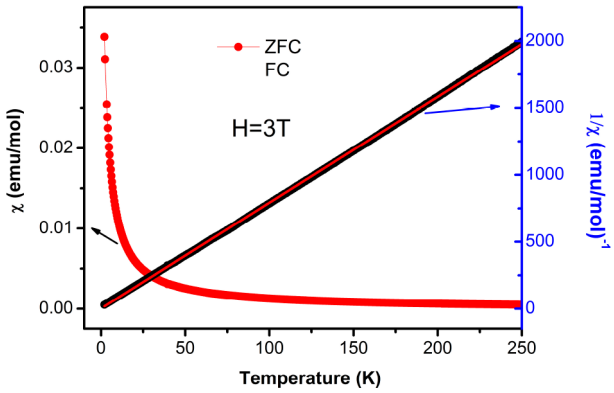

Figure 4. Magnetic susceptibility and its inverse $1/\chi$ as a function of the temperature for the $Ba_2CuO_2Cu_2Se_2$ sample.

formula unit. The Weiss temperature is very close to zero, which hints that the exchange interaction is very weak because of the extremely large length of the Cu−O bond. For $Ba_2CuO_2Cu_2Se_2$, the 3d orbitals of Cu(1) in the $[Cu_2Se_2]$ layer are fully filled; therefore, the effective moment should come from the local moment of Cu(2) in the $[CuO_2]$ plane. The effective magnetic moment, however, is lower than the expected value 1.73 μ_B for the spin $^1/_2$ Cu^{2+}. Therefore, it is suggested that the $[CuO_2]$ plane should be doped with electrons, which is consistent with the results of the calculated oxidation state of Cu(2) by the BVS method. Because the contribution of the $[Cu_2Se_2]$ layer to the susceptibility can be ignored, if there is any magnetic phase transition, it should arise from the Cu(2) ion, with $3d^9$ configured in the $[CuO_2]$ plane. Thus, we can compare the magnetic properties of $Ba_2CuO_2Cu_2Se_2$ with those of other cuprate compounds. In fact, if the antifluorite layers of $[Cu_2Se_2]^{2-}$ in $Ba_2CuO_2Cu_2Se_2$ are replaced with the $[Cl_2]^{2-}$ layers, the forming compounds $A_2CuO_2Cl_2$ (A = Ca, Sr, and Ba) would be the well-known parents of the cuprate superconductors. For $Sr_2CuO_2Cl_2$, its magnetism has been studied by both magnetic susceptibility and NPD. It was reported to be antiferromagnetic with T_N = 251 K identified by NPD, although the antiferromagnetic transition cannot be detected in the susceptibility measurement.[33]

To further clarify whether $Ba_2CuO_2Cu_2Se_2$ undergoes magnetic phase transition, NPD measurements were carried out, as shown in Figure 5. The Rietveld refinement for the

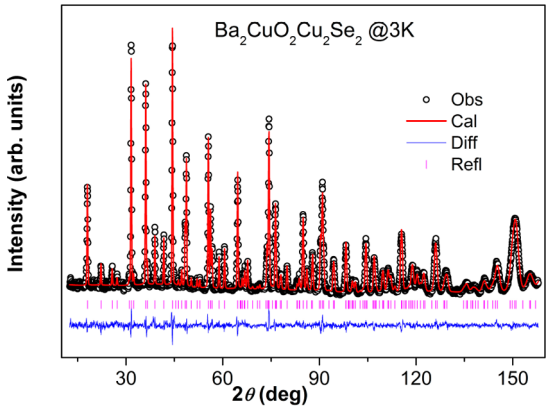

Figure 5. NPD data measured at 3 K for $Ba_2CuO_2Cu_2Se_2$ and its Rietveld refinement.

diffraction pattern measured at 3 K is performed by adopting the same crystal structure. It is converged to R_{wp} = 5.0%, R_p = 4.34%, and χ^2 = 1.2. The crystallographic parameters are shown in Table S2. It demonstrated that the crystal structure is stable in the measured temperature. Compared with the room temperature data, the lattice constant a shrinks only by 0.4%. No magnetic Bragg peak is observed, demonstrating that $Ba_2CuO_2Cu_2Se_2$ does not undergo any magnetic phase transition above 3 K, which is consistent with the small T_{CW} deduced from the susceptibility data.

Reminded by the $[CuO_2]$ planes in $Ba_2CuO_2Cu_2Se_2$, we try to introduce carriers into the system to induce possible superconductivity. Although the samples of $(Ba_{1-x}K_x)_2CuO_2Cu_2Se_2$ with $x < 0.25$ can be synthesized at high pressure, no superconductivity can be found in these samples. For $Ba_2CuO_2Cu_2Se_2$, the bond length is about 2.04 Å, given by half of the lattice constant a, which is larger than the typical cuprate superconductors. For the infinite layer $CaCuO_2$, the bond length is about 1.93 Å,[34] and it is 1.95 Å for the monolayer cuprate $Sr_{2-x}Ba_xCuO_{3+\delta}$ with a T_c value of about 98 K.[35] It is speculated that when the Cu−O bond length is too large, the magnetic interaction would become too weak to give rise to superconductivity. $Ba_2CuO_2Cl_2$ is such a case, where the Cu−O bond length is also about 2.05 Å, and the magnetic transition and superconductivity have not been evidenced.[36]

First-principles calculations were carried out using DFT+U, with an empirical U_{eff} = 7 eV usually adopted for cuprate superconductors.[24] Different magnetic structures were considered including paramagnetic (PM), ferromagnetic, and Néel antiferromagnetic (AFM) states. Our results indicate that AFM has the lowest energy with a small nearest-neighbor (NN) Cu−Cu AFM exchange coupling due to the larger bond length of Cu−O.

The DOS and band structures at ambient pressure are plotted for both the PM and AFM states in Figure 6. The

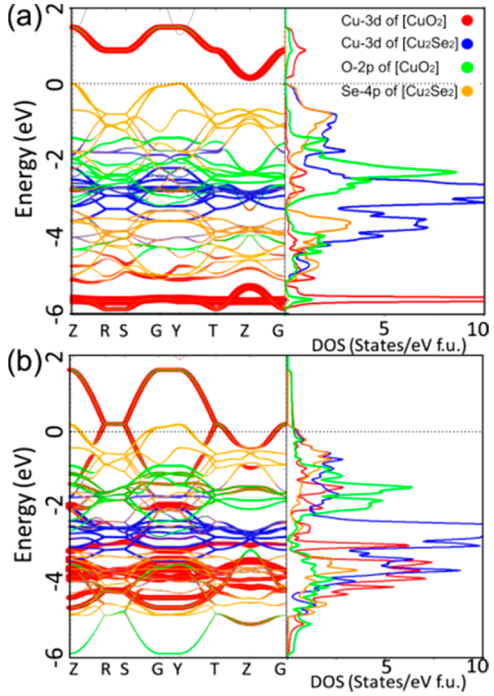

Figure 6. Electronic band structures and partial DOSs calculated by DFT+U for the (a) AFM and (b) PM states.

DOI: 10.1021/acs.inorgchem.8b00171
Inorg. Chem. 2018, 57, 5108−5113

obtained valences of the Cu, O, and Se ions are consistent with experiments. A comparison of the PM and AFM results indicates that AFM correlations may have significant effects on the band structures of the Cu 3d orbitals. While the PM state is metallic, which contradicts with the resistivity measurement, the AFM band structures show a small indirect gap due to splitting of the Cu 3d bands. The top of the valence band and bottom of the conducting band are derived from the Se 4p orbital and upper Hubbard band of the splitting Cu(2) 3d orbital, respectively. The gap value (E_{gap}) is about 0.2 eV for U_{eff} = 7 eV, which is somewhat larger than that deduced from the fitting of our resistivity data. A possible explanation for the observed semiconducting behavior in experiments may be due to two-dimensional AFM fluctuations that have an effect similar to that of the long-range AFM order and cause the gap opening of the half-filled Cu $3d_{x^2-y^2}$ band in the $[CuO_2]$ plane. From the partial DOSs of the $[CuO_2]$ and $[Cu_2Se_2]$ planes, we see a small electron transfer from the Se 4p orbitals to the Cu 3d orbitals of the $[CuO_2]$ plane in the PM state. While this is suppressed in the AFM state, the Se 4p bands remain the closest below the Fermi energy. Thus, hole doping would preferably enter Se 4p orbitals rather than Cu 3d orbitals in the $[CuO_2]$ plane, a situation very different from that for hole-doped cuprates. This explains why the doping in our experiments does not yield superconductivity in this system, even though the crystal structure is similar to that of the usual cuprate superconductors. Another important reason for non-superconducting in doped $Ba_2CuO_2Cu_2Se_2$ is the large bond length of Cu−O, which leads to a much smaller J_{AFM} value of 0.025 eV (2.902×10^2 K) than that of the usual cuprate superconductors (10^3−10^4 K). However, the weak NN coupling may be enhanced under pressure by compressing the crystal lattice. A moderate pressure can usually reduce the lattice constants by 5% for most compounds. That means that, for $Ba_2CuO_2Cu_2Se_2$, the Cu−O band length can be tuned from 2.04 to 1.94 Å, comparable with the $Sr_{2-x}Ba_xCuO_{3+\delta}$ superconductor. At the same time, the pressure can increase the bandwidth and possibly tune the upper Hubbard band to cross the Fermi level. Therefore, pressure may be used to look for superconductivity in the $Ba_2CuO_2Cu_2Se_2$ compound.

CONCLUSION

In summary, the new $Ba_2CuO_2Cu_2Se_2$ compound has been synthesized under high-pressure and high-temperature conditions, which contains alternating $[CuO_2]$ and antifluorite $[Cu_2Se_2]$ layers. It exhibits semiconductor behavior with a low resistivity at room temperature. $Ba_2CuO_2Cu_2Se_2$ does not present magnetic phase transition in the measured temperature range because of the large Cu−O bond length. The first-principles calculations show that the DOS near the top of the valence band is mainly contributed by the Se 4p electrons.

ASSOCIATED CONTENT

Supporting Information

The Supporting Information is available free of charge on the ACS Publications website at DOI: 10.1021/acs.inorgchem.8b00171.

Crystallographic parameters (Tables S1 and S2) and XRD data (Figure S1) (PDF)

AUTHOR INFORMATION

Corresponding Authors

*E-mail: wangxiancheng@iphy.ac.cn (X.W.).
*E-mail: yifeng@iphy.ac.cn (Y.Y.).
*E-mail: jin@iphy.ac.cn (C.J.).

ORCID

Zhaoming Fu: 0000-0002-6697-1630
Xiancheng Wang: 0000-0001-6263-4963
Min Liu: 0000-0002-7674-7309

Author Contributions

X.W. and C.J. conceived the research; W.L. synthesized the sample with the help of J.F.Z. and J.Z.; W.L., M.J., G.Z., and G.D. conducted the measurements of XRD, resistivity, and susceptibility and the refinements of XRD and NPD under the supervision of Z.D., S.Z., and S.F.; Q.H. was responsible for the NPD measurement; W.L., Z.H., H.L., and C.-T.C. conducted the XAS measurement and were responsible for the analysis; Y.Y., Z.F., and M.L. were responsible for the calculations; W.L. and X.W. analyzed the data and wrote the paper with the help of C.J. and Y.Y. All authors discussed the results and commented on the manuscript.

Notes

The authors declare no competing financial interest.

ACKNOWLEDGMENTS

This work was financially supported by the National Science Foundation of China, National Basic Research Program of China.

REFERENCES

(1) Bednorz, J. G.; Muller, K. A. Possible High-Tc Superconductivity in the Ba-La-Cu-O System. *Z. Phys. B: Condens. Matter* **1986**, *64*, 189.
(2) Wu, M. K.; Ashburn, J. R.; Torng, C. J.; Hor, P. H.; Meng, R. L.; Gao, L.; Huang, Z. J.; Wang, Y. Q.; Chu, C. W. Superconductivity at 93-K in a New Mixed-Phase Y-Ba-Cu-O Compound System at Ambient Pressure. *Phys. Rev. Lett.* **1987**, *58*, 908.
(3) Maeda, H.; Tanaka, Y.; Fukutomi, M.; Asano, T. A New High-Tc Oxide Superconductor without a Rare-Earth Element. *Jpn. J. Appl.Phys. Part 2* **1988**, *27*, L209.
(4) Schilling, A.; Cantoni, M.; Guo, J. D.; Ott, H. R. Superconductivity above 130-K in the Hg-Ba-Ca-Cu-O System. *Nature* **1993**, *363*, 56.
(5) Jin, C. Q.; Wu, X. J.; Laffez, P.; Tatsuki, T.; Tamura, T.; Adachi, S.; Yamauchi, H.; Koshizuka, N.; Tanaka, S. Superconductivity at 80 K in $(Sr,Ca)_3Cu2O_{4+\delta}Cl_{2-y}$ Induced by Apical Oxygen Doping. *Nature* **1995**, *375*, 301.
(6) Kamihara, Y.; Watanabe, T.; Hirano, M.; Hosono, H. Iron-based layered superconductor $La[O_{1-x}F_x]FeAs$ (x = 0.05−0.12) with Tc = 26 K. *J. Am. Chem. Soc.* **2008**, *130*, 3296.
(7) Rotter, M.; Tegel, M.; Johrendt, D. Superconductivity at 38 K in the iron arsenide $(Ba_{1-x}K_x)Fe_2As_2$. *Phys. Rev. Lett.* **2008**, *101*, 107006.
(8) Wang, X. C.; Liu, Q. Q.; Lv, Y. X.; Gao, W. B.; Yang, L. X.; Yu, R. C.; Li, F. Y.; Jin, C. Q. The superconductivity at 18 K in LiFeAs system. *Solid State Commun.* **2008**, *148*, 538.
(9) Hsu, F. C.; Luo, J. Y.; Yeh, K. W.; Chen, T. K.; Huang, T. W.; Wu, P. M.; Lee, Y. C.; Huang, Y. L.; Chu, Y. Y.; Yan, D. C.; Wu, M. K. Superconductivity in the PbO-type structure alpha-FeSe. *Proc. Natl. Acad. Sci. U. S. A.* **2008**, *105*, 14262.
(10) Stewart, G. R. Superconductivity in iron compounds. *Rev. Mod. Phys.* **2011**, *83*, 1589.
(11) Jiang, H.; Sun, Y. L.; Xu, Z. A.; Cao, G. H. Crystal chemistry and structural design of iron-based superconductors. *Chin. Phys. B* **2013**, *22*, 087410.
(12) Ogino, H.; Sato, S.; Kishio, K.; Shimoyama, J.; Tohei, T.; Ikuhara, Y. Homologous series of iron pnictide oxide superconductors

DOI: 10.1021/acs.inorgchem.8b00171
Inorg. Chem. 2018, 57, 5108−5113

(Fe_2As_2) [$Ca_{n+1}(Sc,Ti)_nO_y$] (n = 3,4,5) with extremely thick blocking layers. *Appl. Phys. Lett.* **2010**, *97*, 072506.
(13) Zhu, X. Y.; Han, F.; Mu, G.; Zeng, B.; Cheng, P.; Shen, B.; Wen, H. H. $Sr_3Sc_2Fe_2As_2O_5$ as a possible parent compound for FeAs-based superconductors. *Phys. Rev. B: Condens. Matter Mater. Phys.* **2009**, *79*, 024516.
(14) Zhu, W. J.; Hor, P. H. Crystal structure of new layered oxysulfides: $Sr_2Cu_2Fe_2O_5S_2$ and Sr_2CuMO_3S (M = Cr, Fe, In). *J. Solid State Chem.* **1997**, *134*, 128.
(15) Zhu, W. J.; Hor, P. H.; Jacobson, A. J.; Crisci, G.; Albright, T. A.; Wang, S. H.; Vogt, T. $A_2Cu_2CoO_2S_2$ (A = Sr, Ba), a novel example of a square-planar CoO_2 layer. *J. Am. Chem. Soc.* **1997**, *119*, 12398.
(16) Otzschi, K.; Ogino, H.; Shimoyama, J.; Kishio, K. New candidates for superconductors; A series of layered oxysulfides $(Cu_2S_2)(Sr_{n+1}M_nO_{3n-1})$. *J. Low Temp. Phys.* **1999**, *117*, 729.
(17) Zhang, H.; Jin, S. F.; Guo, L. W.; Shen, S. J.; Lin, Z. P.; Chen, X. L. Bandgap narrowing in the layered oxysulfide semiconductor $Ba_3Fe_2O_5Cu_2S_2$: Role of FeO_2 layer. *Chin. Phys. B* **2016**, *25*, 026101.
(18) Smura, C. F.; Parker, D. R.; Zbiri, M.; Johnson, M. R.; Gal, Z. A.; Clarke, S. J. High-Spin Cobalt(II) Ions in Square Planar Coordination: Structures and Magnetism of the Oxysulfides $Sr_2CoO_2Cu_2S_2$ and $Ba_2CoO_2Cu_2S_2$ and Their Solid Solution. *J. Am. Chem. Soc.* **2011**, *133*, 2691.
(19) Jin, S. F.; Chen, X. L.; Guo, J. G.; Lei, M.; Lin, J. J.; Xi, J. G.; Wang, W. J.; Wang, W. Y. $Sr_2Mn_3Sb_2O_2$ Type Oxyselenides: Structures, Magnetism, and Electronic Properties of $Sr_2AO_2M_2Se_2$ (A = Co, Mn; M = Cu, Ag). *Inorg. Chem.* **2012**, *51*, 10185.
(20) Chou, T. L.; Mustonen, O.; Tripathi, T. S.; Karppinen, M. Isovalent Ca and Ba substitutions in thermoelectric layer-structured oxyselenide $Sr_2CoO_2Cu_2Se_2$. *J. Phys.: Condens. Matter* **2016**, *28*, 035802.
(21) Park, Y. B.; Degroot, D. C.; Schindler, J. L.; Kannewurf, C. R.; Kanatzidis, M. G. Intergrowth of 2 Different Layered Networks in the Metallic Copper Oxyselenide $Na_{1.9}Cu_2Se_2Cu_2O$. *Chem. Mater.* **1993**, *5*, 8.
(22) Zhang, J.; Su, R.; Wang, X. C.; Li, W. M.; Zhao, J. F.; Deng, Z.; Zhang, S. J.; Feng, S. M.; Liu, Q. Q.; Zhao, H. Z.; Guan, P. F.; Jin, C. Q. Synthesis, crystal structures, and electronic properties of one dimensional $Ba_9Sn_3(Te_{1-x}Se_x)_{15}$ (x = 0−1). *Inorg. Chem. Front.* **2017**, *4*, 1337.
(23) Blaha, P.; Schwarz, K.; Madsen, G. K. H.; Kvasnicka, D.; Luitz, J. *WIEN2K, User's Guide*; Technische Universitat Wien: Vienna, Austria, 2001; http://www.wien2k.at/reg_user/textbooks/usersguide.pdf.
(24) Blaha, P.; Schwarz, K.; Novak, P. Electric field gradients in cuprates: Does LDA+U give the correct charge distribution? *Int. J. Quantum Chem.* **2005**, *101*, 550.
(25) Brock, S. L.; Kauzlarich, S. M. $A_2Zn_3As_2O_2$ (A = Ba, Sr) - a Rare Example of Square-Planar Zinc. *Inorg. Chem.* **1994**, *33* (11), 2491.
(26) Herkelrath, S. J. C.; Saratovsky, I.; Hadermann, J.; Clarke, S. J. Fragmentation of an Infinite ZnO2 Square Plane into Discrete [ZnO2](2-) Linear Units in the Oxyselenide $Ba_2ZnO_2Ag_2Se_2$. *J. Am. Chem. Soc.* **2008**, *130* (44), 14426.
(27) Zhou, T. T.; Wang, Y. M.; Jin, S. F.; Li, D. D.; Lai, X. F.; Ying, T. P.; Zhang, H.; Shen, S. J.; Wang, W. J.; Chen, X. L. Structures and Physical Properties of Layered Oxyselenides $Ba_2MO_2Ag_2Se_2$ (M = Co, Mn). *Inorg. Chem.* **2014**, *53* (8), 4154.
(28) Huang, M. J.; Deng, G.; Chin, Y. Y.; Hu, Z.; Cheng, J. G.; Chou, F. C.; Conder, K.; Zhou, J. S.; Pi, T. W.; Goodenough, J. B.; Lin, H. J.; Chen, C. T. Determination of hole distribution in $Sr_{14-x}Ca_xCu_{24}O_{41}$ using soft x-ray absorption spectroscopy at the Cu *L*-3 edge. *Phys. Rev. B: Condens. Matter Mater. Phys.* **2013**, *88*, 014520.
(29) Chen, C. T.; Tjeng, L. H.; Kwo, J.; Kao, H. L.; Rudolf, P.; Sette, F.; Fleming, R. M. Out-of-Plane Orbital Characters of Intrinsic and Doped Holes in $La_{2-X}Sr_xCuO_4$. *Phys. Rev. Lett.* **1992**, *68*, 2543.
(30) Tjeng, L. H.; Chen, C. T.; Cheong, S. W. Comparative soft x-ray resonant-photoemission study on $Bi_2Sr_2CaCu_2O_8$, CuO and Cu_2O. *Phys. Rev. B: Condens. Matter Mater. Phys.* **1992**, *45*, 8205.
(31) Chen, C. L.; Yeh, K. W.; Huang, D. J.; Hsu, F. C.; Lee, Y. C.; Huang, S. W.; Guo, G. Y.; Lin, H. J.; Rao, S. M.; Wu, M. K. Orbital polarization of the unoccupied states in multiferroic $LiCu_2O_2$. *Phys. Rev. B: Condens. Matter Mater. Phys.* **2008**, *78*, 214105.
(32) Tan, S. G.; Shao, D. F.; Lu, W. J.; Yuan, B.; Liu, Y.; Yang, J.; Song, W. H.; Lei, H. C.; Sun, Y. P. CuSe-based layered compound $Bi_2YO_4Cu_2Se_2$ as a quasi-two-dimensional metal. *Phys. Rev. B: Condens. Matter Mater. Phys.* **2014**, *90*, 085144.
(33) Vaknin, D.; Sinha, S. K.; Stassis, C.; Miller, L. L.; Johnston, D. C. Antiferromagnetism in $Sr_2CuO_2Cl_2$. *Phys. Rev. B: Condens. Matter Mater. Phys.* **1990**, *41*, 1926.
(34) Siegrist, T.; Zahurak, S. M.; Murphy, D. W.; Roth, R. S. The Parent Structure of the Layered High-Temperature Superconductors. *Nature* **1988**, *334*, 231.
(35) Gao, W. B.; Liu, Q. Q.; Yang, L. X.; Yu, Y.; Li, F. Y.; Jin, C. Q.; Uchida, S. Out-of-plane effect on the superconductivity of $Sr_{2-x}Ba_xCuO_{3+\delta}$with T_c up to 98 K. *Phys. Rev. B: Condens. Matter Mater. Phys.* **2009**, *80*, 094523.
(36) Tatsuki, T.; TokiwaYamamoto, A.; Tamura, T.; Moriwaki, Y.; Wu, X. J.; Adachi, S.; Tanabe, K. A new oxychloride, $Ba_2CuO_2Cl_2$, prepared under high pressure. *Phys. C* **1996**, *265*, 323.

DOI: 10.1021/acs.inorgchem.8b00171
Inorg. Chem. 2018, 57, 5108−5113